

# Demand Driven Deployment Capabilities in Cyclus, a Fuel Cycle Simulator

Gwendolyn J. Chee<sup>a</sup>, Roberto E. Fairhurt Agosta<sup>a</sup>, Jin Whan Bae<sup>b</sup>, Robert R. Flanagan<sup>c</sup>, Anthony Scopatz<sup>c</sup>, Kathryn D. Huff<sup>a,\*</sup>

<sup>a</sup>*Dept. of Nuclear, Plasma, and Radiological Engineering, University of Illinois at Urbana-Champaign, Urbana, IL 61801*

<sup>b</sup>*Oak Ridge National Laboratory, Oak Ridge, TN, United States*

<sup>c</sup>*Nuclear Engineering Program, University of South Carolina*

---

## Abstract

The present United States nuclear fuel cycle faces challenges that hinder the expansion of nuclear energy technology. The U.S. Department of Energy identified four nuclear fuel cycle options we could transition to, which would make nuclear energy technology more desirable. To successfully analyze the transition from our current fuel cycle to these promising fuel cycles, we need a nuclear fuel cycle simulator that can predictively and automatically deploy fuel cycle facilities to meet user-defined power demand. In this work, we developed demand-driven deployment capabilities in CYCLUS, a nuclear fuel cycle simulator. User-controlled capabilities such as supply buffers, facility preferences, prediction algorithms, and installed capacity deployment were introduced to give users tools to minimize power undersupply in a transition scenario simulation. We demonstrate `d3ploy`'s capability to automatically deploy fuel cycle facilities to set up transition scenarios for promising nuclear fuel cycle options.

*Keywords:* nuclear fuel cycle, python, time series forecasting

---

\*Corresponding Author

*Email address:* `kdhuff@illinois.edu` (Kathryn D. Huff)

## 1. Introduction

Nuclear Fuel Cycle (NFC) simulators are system analysis tools used to evaluate quantitative measures of dynamic NFC performance in both high and low resolution. Plutonium concentration in a single used fuel bundle and total electricity produced are examples of high and low resolution elements, respectively. The primary purpose of NFC simulators is to understand the dependence between various input parameters and components in the NFC and the impact their variations have on the system’s performance. The results of NFC simulators are used to guide research efforts, advise future design choices, and provide decision-makers with a transparent tool for evaluating Fuel Cycle Options (FCO) to inform big-picture policy decisions [1].

Many fuel cycle simulators, automatically deploy reactor facilities to meet a user-defined power demand. However, the user must define a deployment scheme of supporting facilities to avoid gaps in the supply chain resulting in idle reactor capacity. To avoid this issue, some users choose to set infinite capacity for supporting facilities but this is an inaccurate representation of reality resulting in misrepresented results. It is straightforward to manually determine a deployment scheme for a once-through fuel cycle, however, it is not straightforward for complex closed fuel cycle scenarios. To ease setting up realistic NFC simulations, a NFC simulator should bring demand-responsive deployment decisions into the simulation logic dynamics [2]. Thus, a next-generation NFC simulator should predictively and automatically deploy fuel cycle facilities to meet a user-defined power demand.

In CYCLUS, an agent-based nuclear fuel cycle simulation framework [3], each entity (i.e. **Region**, **Institution**, or **Facility**) in the fuel cycle is an agent. **Region** agents represent geographical or political areas that **Institution** and **Facility** agents reside. **Institution** agents control the deployment and decommissioning of **Facility** agents and represent legal operating organizations such as utilities, governments, etc. [3]. **Facility** agents represent nuclear fuel cycle facilities such as mines, conversion facilities, reactors, reprocessing

facilities, etc. CYCAMORE [4] provides basic CYCLUS' **Region**, **Institution**, and **Facility** archetypes.

### 1.1. Context of Work

The impact of climate change on natural and human systems is increasingly  
35 apparent. The production and use of energy contribute to two-thirds of the total  
Green House Gas (GHG) emissions [5]. Furthermore, as the human population  
increases and previously under-developed nations urbanize rapidly, global energy  
demand is forecasted to increase. The types of power generation technologies  
used will heavily impact the effects of growing energy demand on climate change.  
40 Large scale deployment of nuclear power plants has significant potential to reduce  
GHG production due to their low carbon emissions [5].

However, the nuclear power industry is facing four major challenges of large  
scale nuclear power deployment: cost, safety, proliferation, and waste [6]. Nuclear  
power has high overall lifetime costs and increases risks of nuclear proliferation.  
45 There is also an unresolved long-term nuclear waste management strategy and  
perceived adverse safety, environmental, and health effects [6]. The nuclear  
power industry must overcome these four challenges to ensure continued global  
use and expansion of nuclear energy technology.

The four challenges described above are associated with the present once-  
50 through fuel cycle in the United States (US), in which fabricated nuclear fuel  
is used once and placed into storage to await disposal. An evaluation and  
screening study of a comprehensive set of nuclear fuel cycle options [7] was  
conducted to assess for performance improvements compared with the existing  
once-through fuel cycle (EG01) in the US across a wide range of criteria. Fuel  
55 cycles that involved continuous recycling of co-extracted U/Pu or U/TRU in  
fast spectrum critical reactors consistently scored high on overall performance.  
Table 1 describes these fuel cycles: EG23, EG24, EG29, and EG30.

The evaluation and screening study assumed the nuclear energy systems  
were at equilibrium to understand the end-state benefits of each Evaluation  
60 Group (EG) [8]. In this work, our goal is to model the transition from the

| Fuel Cycle               | Open or Closed | Fuel Type                     | Reactor Type                     |
|--------------------------|----------------|-------------------------------|----------------------------------|
| <b>EG01</b><br>(current) | Open           | Enriched-U                    | Thermal Critical                 |
| <b>EG23</b>              | Closed         | Recycled U/Pu<br>+ Natural-U  | Fast Critical                    |
| <b>EG24</b>              | Closed         | Recycled U/TRU<br>+ Natural-U | Fast Critical                    |
| <b>EG29</b>              | Closed         | Recycled U/Pu<br>+ Natural-U  | Fast Critical & Thermal Critical |
| <b>EG30</b>              | Closed         | Recycled U/TRU<br>+ Natural-U | Fast Critical & Thermal Critical |

**Table 1:** Descriptions of the current and other high performing nuclear fuel cycle evaluation groups described in the evaluation and screening study [7].

initial EG01 state to these promising future end-states. To successfully analyze time-dependent transition scenarios, the NFC simulator tool must automate the transition scenario simulation setup. Therefore, the Demand-Driven CYCAMORE Archetypes project (NEUP-FY16-10512) was initiated to develop demand-driven deployment capabilities in CYCLUS. This capability, `d3ploy`, is a CYCLUS **Institution** agent that deploys facilities to meet user-defined power demand.

### 1.2. Novelty

We utilized time series forecasting methods to effectively predict future commodity supply and demand in `d3ploy`. Solar and wind power generation commonly use these methods to make future predictions based on past time series data [9, 10, 11, 12]. This is a novel approach that has never been applied to NFC simulators.

### 1.3. Objectives

The main objectives of this paper are: (1) to describe the demand-driven deployment capabilities in CYCLUS, (2) to describe the prediction methods available in `d3ploy`, and (3) to demonstrate the use of `d3ploy` in setting up

EG01-23, EG01-24, EG01-29, and EG01-30 transition scenarios with various power demand curves.

## 2. Methodology

80 In CYCLUS, developers have the option to design agents using C++ or Python. The `d3ploy Institution` agent was implemented in Python to enable the use of well-developed time series forecasting Python packages.

In a CYCLUS NFC simulation, at every time step, `d3ploy` predicts the supply and demand of each commodity for the next time step. When there exists 85 undersupply for any commodity, `d3ploy` deploys facilities to meet its predicted demand. Figure 1 shows the logic flow of `d3ploy` at every time step.

`d3ploy` aims to minimize the undersupply of power (Equation 1).

$$obj = \min \sum_{t=1}^{t_{end}} |D_{t,power} - S_{t,power}| \quad (1)$$

The sub-objectives are (1) to minimize the number of time steps of undersupply or under-capacity of any commodity:

$$obj = \min \sum_{i=c_1}^{c_M} \sum_{t=1}^{t_N} |D_{t,i} - S_{t,i}|, \quad (2)$$

(2) to minimize excessive oversupply of all commodities:

$$obj = \min \sum_{i=c_1}^{c_M} \sum_{t=1}^{t_N} |S_{t,i} - D_{t,i}|. \quad (3)$$

where:

$D$  = Demand

$S$  = Supply

$c$  = Commodity type

$M$  = Number of commodities

$N$  = Number of time steps

Minimizing excessive oversupply reflects reality in which utilities avoid undersupply of power on the grid by ensuring power plants are never short of fuel while

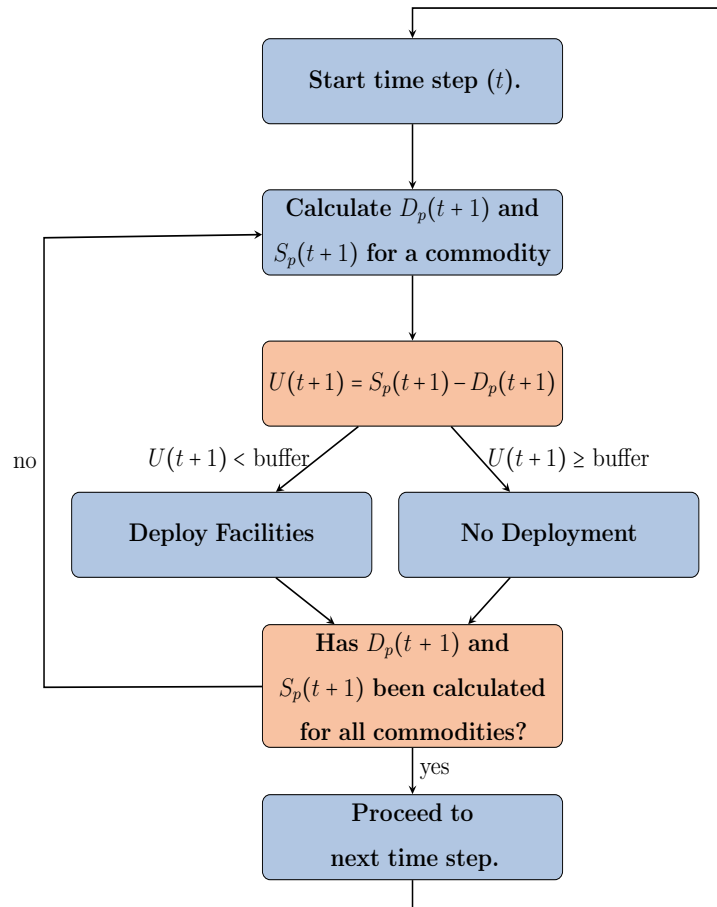


**Figure 1:** d3ploy logic flow at every time step in CYCLUS [13].

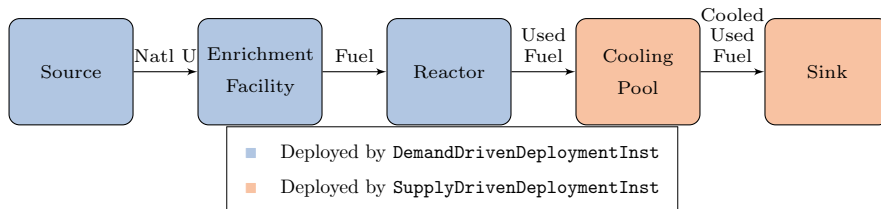


**Figure 2:** Simple once-through fuel cycle depicting which facilities are deployed by `DemandDrivenDeploymentInst` and `SupplyDrivenDeploymentInst`.

avoiding expensive oversupply. NFC simulators often face power undersupplies  
 90 due to lack of viable fuel, despite having sufficient installed reactor capacity. Using `d3ploy` to automate the deployment of supporting facilities prevents this.

### 2.1. Structure

In `d3ploy`, two distinct institutions control front-end and back-end fuel cycle facilities: `DemandDrivenDeploymentInst` and `SupplyDrivenDeploymentInst`,  
 95 respectively. The reason for this distinction is that front-end facilities meet the demand for commodities they produce, whereas back-end facilities meet supply for the commodities they demand. For example, when a reactor facility demands fuel, `DemandDrivenDeploymentInst` deploys fuel fabrication facilities to create fuel supply. For back-end facilities, the reactor generates spent fuel,  
 100 and `SupplyDrivenDeploymentInst` deploys waste storage facilities to create capacity to store the spent fuel. Figure 2 depicts a simple once-through fuel cycle and the `Institution` type governing each facility’s deployment.

#### 2.1.1. Deployment Driving Method

The user may deploy facilities based on the difference between predicted  
 105 demand and predicted supply, *or* predicted demand and installed capacity. Using installed capacity instead of predicted supply has two advantages. First, to prevent over-deployment of facilities with an intermittent supply such as reactors that require refueling. If predicted supply is selected instead of installed capacity, `d3ploy` will deploy surplus reactors during refueling downtimes to

110 meet the temporary power undersupply. Second, to prevent infinite deployment  
of a facility that demands a commodity no longer available in the simulation.  
For example, a reprocessing plant that fabricates Sodium-Cooled Fast Reactor  
(SFR) fuel might demand Pu after depletion of the existing Pu inventory and  
decommissioning of the LWR reactors that produce it, resulting in infinite  
115 deployment of reprocessing facilities in a futile attempt to produce SFR fuel.

## 2.2. *Input Variables*

Table 2 lists and gives examples of the input variables `d3ploy` accepts. The  
user must do the following: define the facilities in the simulation, their respective  
capacities, the demand driving commodity, its demand equation, the deployment  
120 driving method, and prediction method. The user also has the option to define  
supply/capacity buffers for individual commodities, facility preferences, and  
facility fleet shares. The subsequent sections describes the buffers, facility  
preferences, and prediction methods.

### 2.2.1. *Supply/Capacity Buffer*

125 In `DemandDrivenDeploymentInst`, the user has the option to specify a supply  
buffer for each commodity; `d3ploy` accounts for the buffer when calculating pre-  
dicted demand and deploys facilities accordingly. In `SupplyDrivenDeployment  
Inst`, the user has the option to specify a capacity buffer for specific commodities;  
`d3ploy` accounts for the buffer when calculating predicted supply and deploys  
130 facilities accordingly. The buffer is defined as a percentage (equation 4) or  
absolute value (equation 5).

$$S_{pwb} = S_p(1 + d) \tag{4}$$

$$S_{pwb} = S_p + a \tag{5}$$



|                 | <b>Input Parameter</b>       | <b>Examples</b>                                                                     |
|-----------------|------------------------------|-------------------------------------------------------------------------------------|
| <b>Required</b> | Demand driving commodity     | Power                                                                               |
|                 | Demand equation              | $P(t) = 10000, \sin(t), 10000*t$                                                    |
|                 | Facilities it controls       | Fuel Fab, LWR reactor, Sink, etc.                                                   |
|                 | Capacities of the facilities | 3000 kg, 1000 MW, 50000 kg                                                          |
|                 | Prediction method            | Power: fast fourier transform<br>Fuel: moving average<br>Spent fuel: moving average |
|                 | Deployment driven by         | Installed Capacity                                                                  |
| <b>Optional</b> | Supply/Capacity Buffer type  | Absolute                                                                            |
|                 | Supply/Capacity Buffer size  | Power: 3000 MW<br>Fuel: 0 kg<br>Spent fuel: 0 kg                                    |
|                 | Facility preferences         | LWR reactor = 100-t<br>SFR reactor = t-100                                          |
|                 | Fleet share percentage       | MOX LWR = 85%<br>SFR = 15%                                                          |

**Table 2:** d3p1oy’s required and optional input parameters with examples.

where:

$S_{pwb}$  = predicted supply/capacity with buffer

$S_p$  = predicted supply/capacity without buffer

$d$  = percentage value in decimal form

$a$  = absolute value of the buffer

For example, the user sets the power commodity’s absolute supply buffer to be 2000 MW and predicted demand is 10000 MW, d3p1oy deploys reactor facilities to meet the predicted demand and supply buffer, resulting in a power supply of:

$$S_{pwb} = S_p + a$$

$$\begin{aligned} S_{pwb} &= 10000\text{MW} + 2000\text{MW} \\ &= 12000\text{MW} \end{aligned}$$

Using a combination of the buffer capability and installed capacity deployment

driving method in a transition scenario simulation effectively minimizes under-  
supply of a commodity while avoiding excessive oversupply. This is demonstrated  
135 in section 3.1.

### *2.3. Facility Preference and Fleet Share*

The user has the option to give preferences to facilities' that supply the same  
commodity. These preferences are in the form of a time-dependent equation so  
that the preferences can be dynamic with time. `d3ploy` uses these equations  
140 to determine which facility to deploy during a commodity shortage. In table  
2, the Light Water Reactor (LWR) reactor has a preference of  $100 - t$ , and the  
Sodium-Cooled Fast Reactor (SFR) reactor has a preference of  $t - 100$ . At time  
step 1, LWR preference is 99, while SFR preference is -99; therefore a LWR is  
deployed if there is a commodity shortage. At time step 105, LWR preference is  
145 -5, while SFR preference is 5; therefore a SFR is deployed if there is a commodity  
shortage.

The user also has the option to specify percentage-share for facilities that  
provide the same commodity. In table 2, the mixed oxide (MOX) LWR has a  
share of 85%, while the SFR has a share of 15%. This constrains SFR deployment  
150 to 85% of total power demand and MOX LWR deployment to 15% of total power  
demand.

The year the transition begins is selected by customizing facility preferences  
to begin preference for advanced reactors at a certain year, and the sharing  
capability determines the percentage share of each type of reactor to transition  
155 to. Therefore, when `d3ploy` predicts an undersupply of a commodity it deploys  
facilities in order of preference, starting at the highest and moving down if  
the facility percentage share is already met. If a facility type does not have  
any preferences, `d3ploy` deploys available facilities to minimize the number of  
deployed facilities and oversupply of the commodity.

### *2.4. Prediction Methods*

`d3ploy` records supply and demand values at each time step for all commodi-  
ties to provide time-series data for `d3ploy`'s time series forecasting methods to

predict future supply and demand for each commodity. The time series forecasting methods investigated include non-optimizing, deterministic-optimizing, and stochastic-optimizing methods. Non-optimizing methods are techniques that harness simple moving average and autoregression concepts which use historical data to infer future supply and demand values. Deterministic-optimizing and stochastic-optimizing methods are techniques that use an assortment of more sophisticated time series forecasting concepts to predict future supply and demand values. Deterministic-optimizing methods give deterministic solutions, while stochastic-optimizing methods give stochastic solutions.

Depending on the scenario in question, each forecasting method offers distinct benefits and disadvantages. The various methods are compared for each type of simulation to determine the most effective prediction method for a given scenario. The following sections describe the prediction methods.

#### 2.4.1. Non-Optimizing Methods

Non-optimizing methods include: Moving Average (MA), Autoregressive Moving Average (ARMA), and Autoregressive Heteroskedasticity (ARCH). The MA method calculates the average of a user-defined number of previous entries in a commodity's time series and returns it as the predicted value (equation 6).

$$\text{Predicted Value} = \frac{V_1 + V_2 + \dots + V_n}{n} \quad (6)$$

The ARMA method combines moving average and autoregressive models (equation 7). The first term is a constant, second term is white noise, the third term is the autoregressive model, and the fourth term is the moving average model. The ARMA method is more accurate than the MA method because of the inclusion of the autoregressive term.

$$X_t = c + \epsilon_t + \sum_{i=1}^p \varphi_i X_{t-i} + \sum_{i=1}^q \theta_i \epsilon_{t-i} \quad (7)$$

The ARCH method modifies the original moving average term (described in equation 7). This modification makes the ARCH method better than the ARMA

method for volatile time-series data [14]. The StatsModels [15] Python package is used to implement ARMA and ARCH methods in `d3ploy`.

#### 190 2.4.2. Deterministic-Optimizing Methods

Deterministic methods include Fast Fourier Transform (FFT), Polynomial Fit (POLY), Exponential Smoothing (EXP-SMOOTHING), and Triple Exponential Smoothing (HOLT-WINTERS). The FFT method computes the discrete Fourier transform of the time series to predict future demand and supply values (equation 8). This method is implemented in `d3ploy` using the SciPy [16] Python package.

$$X_k = \sum_{n=0}^{N-1} x_n e^{-i2\pi kn/N} \quad (8)$$

The POLY method models the time series data with a user-defined  $n$ th degree polynomial to determine future demand and supply values. This method was implemented in `d3ploy` using the NumPy [17] Python package. The EXP-SMOOTHING and HOLT-WINTERS methods use a weighted average of time-series data with exponentially decaying weights for older time series values [18] to create a model to determine future demand and supply values. The EXP-SMOOTHING method excels in modeling univariate time series data without trend or seasonality, whereas the HOLT-WINTERS method applies exponential smoothing three times, resulting in higher accuracy when modeling seasonal time series data. The StatsModels [15] Python package was used to implement both of these methods in `d3ploy`.

#### 205 2.5. Stochastic-Optimizing Methods

There is one stochastic-optimizing method: step-wise seasonal method (SW-SEASONAL). The method was implemented in `d3ploy` by the auto Autoregressive Integrated Moving Averages (ARIMA) method in the pmdarima [19] Python package. The ARIMA model is a generalization of the Autoregressive Moving Average (ARMA) model to make the model fit the time series data better.

### 3. Results

To demonstrate `d3ploy`'s capability conduct transition scenario analysis effectively and meet the objectives described in section 1.3, this section (1) demonstrates `d3ploy`'s capability in simple transition scenarios, (2) compares the use of different prediction methods in EG01-EG23, EG01-EG24, EG01-EG29, and EG01-EG30 transition scenarios, and (3) demonstrates successful `d3ploy` setup of EG01-EG23, EG01-EG24, EG01-EG29, and EG01-EG30 transition scenarios. The input files and scripts to reproduce the results and plots in this paper are found in [20] and [21].

#### 3.1. Demonstration of `d3ploy`'s capabilities

We conducted a simple transition scenario simulation with linearly increasing power demand to demonstrate `d3ploy`'s capabilities and inform input parameter choices when setting up complex many-facility transition scenarios. This simulation only includes three facility types: `source`, `reactor`, and `sink`. The simulation begins with ten `reactor` facilities (`reactor1` to `reactor10`). These reactors have staggered cycle lengths and lifetimes to prevent simultaneous refueling and setup gradual decommissioning. `d3ploy` is configured to deploy `new reactor` facilities to meet the loss of power supply created by the decommissioning of the initial `reactor` facilities. Table 3 shows the `d3ploy` input parameters for this simulation.

Figures 3a, 3b, and 3c demonstrate `d3ploy`'s capability to deploy reactor and supporting facilities to meet the linearly increasing power demand and subsequently demanded secondary commodities with minimal undersupply. In Figure 3a there exists no time steps in which the supply of power falls under demand, meeting the main objective of `d3ploy`. By using a combination of the FFT method for predicting demand and a power supply buffer of 2000MW (the capacity of 2 reactors), we minimized the number of undersupplied time steps for every commodity.

In figure 3b, a large-throughput source facility is initially deployed to meet the large initial fuel demand for the commissioning of ten reactors. By having a

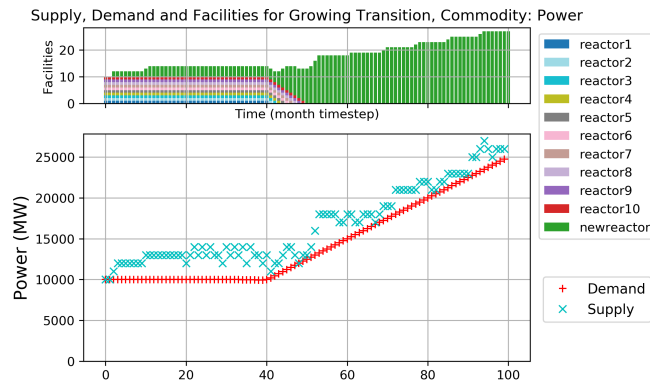
|                 | <b>Input Parameters</b>   | <b>Simple Transition Scenario</b>        |
|-----------------|---------------------------|------------------------------------------|
| <b>Required</b> | Demand driving commodity  | Power                                    |
|                 | Demand equation [MW]      | $t < 40 = 1000, t \geq 40 = 1000 + 250t$ |
|                 | Available facilities      | Source, Reactor, Sink                    |
|                 | Prediction method         | FFT                                      |
|                 | Deployment driving method | Installed Capacity                       |
| <b>Optional</b> | Buffer type               | Absolute                                 |
|                 | Buffer size               | Power: 2000MW, Fuel: 1000kg              |

**Table 3:** `d3ploy`'s input parameters for the simple transition scenario with linearly increasing power demand.

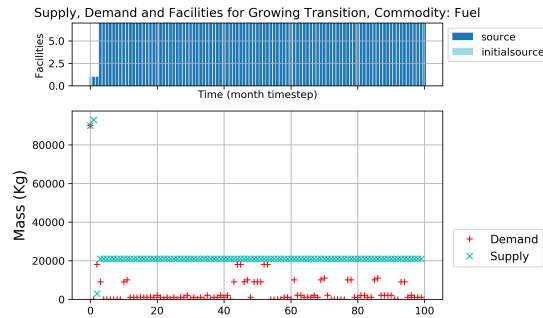
large-throughput source facility exist for the first few time steps, `d3ploy` does not deploy supporting facilities that become redundant at later times in the simulation. This reflects reality in which reactor manufacturers accumulate an appropriate amount of fuel inventory before starting up reactors. There is one time step in which a power undersupply exists after the decommissioning of the large initial facility; this is unavoidable as the prediction methods in `d3ploy` are unable to foresee this sudden drop in demand.

### 3.2. Comparison of Prediction Methods

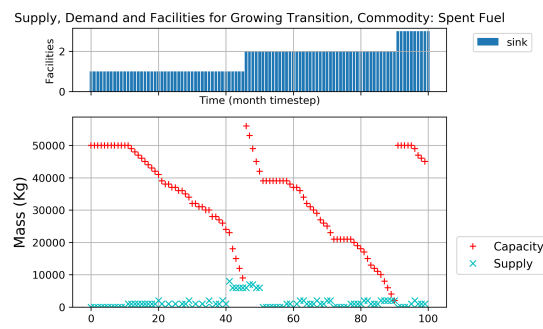
EG01-EG23, EG01-EG24, EG01-EG29, and EG01-EG30 transition scenarios are set up in `CYCLUS` using `d3ploy`. EG01-23 and EG01-29 transition scenario simulations have a constant power demand, while EG01-24 and EG01-30 have a linearly increasing power demand. We identified the most effective `d3ploy` prediction method for each scenario by comparing the results of using each prediction method in each scenario. Similar to the simple transition scenario, these transition scenario simulations begin with an initial fleet of LWRs that start progressively decommissioning at the 80-year mark, after which `d3ploy` deploys SFRs and MOX LWRs to meet the power demand. Figure 4 shows the setup of facilities and mass flows for EG01-23 and EG01-29 in `CYCLUS`. In



(a) Power demand is a user-defined equation and power is supplied by the reactors. There are no time steps with undersupply of power.



(b) Fuel is demanded by reactors and supplied by source facilities. There is only one time step with undersupply of fuel.



(c) Spent Fuel is supplied by reactors and the capacity is provided by sink facilities. There are no time steps with under-capacity of sink space.

**Figure 3:** Simple linearly increasing power demand transition scenario with three facility types: source, reactor, and sink.

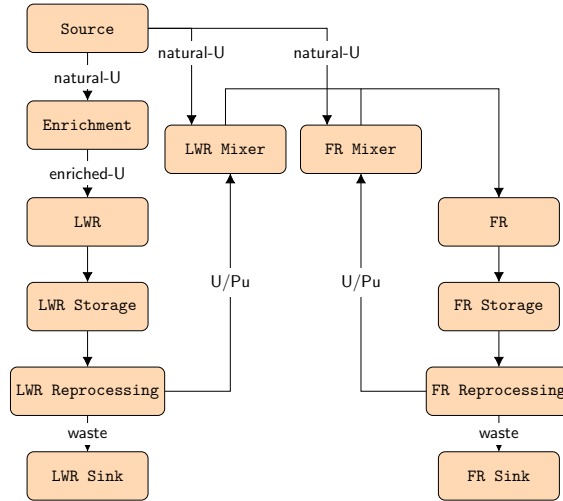
EG01-23 and EG01-29, recycled plutonium from LWR spent fuel produces SFR fuel. EG01-24 and EG01-30 are similar to EG01-23 and EG01-29, respectively, with the exception that all transuranic elements are recycled.

In Figure 5, crosses represent the time steps in which there exists undersupply or under-capacity of each commodity for the constant power EG01-23 transition scenario. The size of the crosses are proportional to the undersupply value. Table 7 shows the number of time steps with power undersupply for constant power EG01-EG23 and EG01-29, linearly increasing power EG01-24 and EG01-30 transition scenarios. Figure 5 demonstrates that the POLY and FFT methods perform the best for the EG01-23 transition scenario, with the least number of points on the plot, indicating they have the fewest number of time steps with undersupply and under-capacity of commodities. Table 7 shows that the POLY method performs slightly better at minimizing undersupply of power than the FFT method, with only 6 power undersupplied time steps. We conducted a similar analysis for the constant power EG01-29 scenario, and as seen in Table 7, the POLY prediction method also performed best for minimizing undersupply of power.

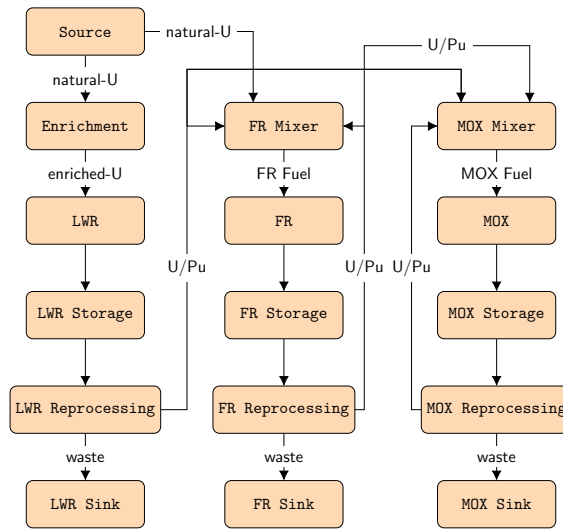
In Figure 6, crosses represent the time steps in which there exists undersupply or under-capacity of each commodity for a linearly increasing power EG01-24 transition scenario. Figure 6 demonstrates that the FFT method performs the best at minimizing the undersupply of all commodities. We conducted a similar analysis for the constant power EG01-30 scenario, and as seen in Table 7, the FFT prediction method also performed best for minimizing undersupply of power.

From Figures 5, 6, and Table 7, we can see that the POLY method performs best for constant power transition scenarios, and the FFT method performs best for linearly increasing power transition scenarios. Undersupply and under-capacity of commodities occur during two main time periods: initial demand for the commodity and during the transition period. To further d3ploy's primary objective of minimizing the power undersupply, sensitivity analysis of the power supply buffer is conducted with the best-performing prediction method for each transition scenario.





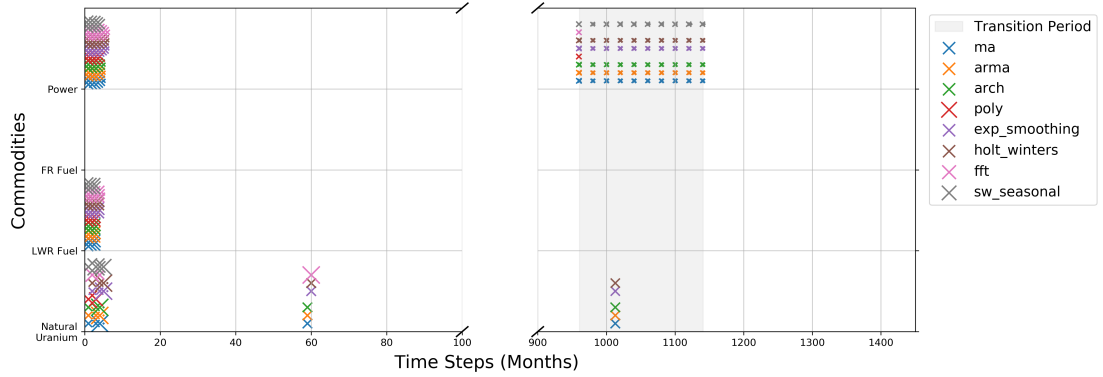
(a) EG01-EG23.



(b) EG01-EG29.

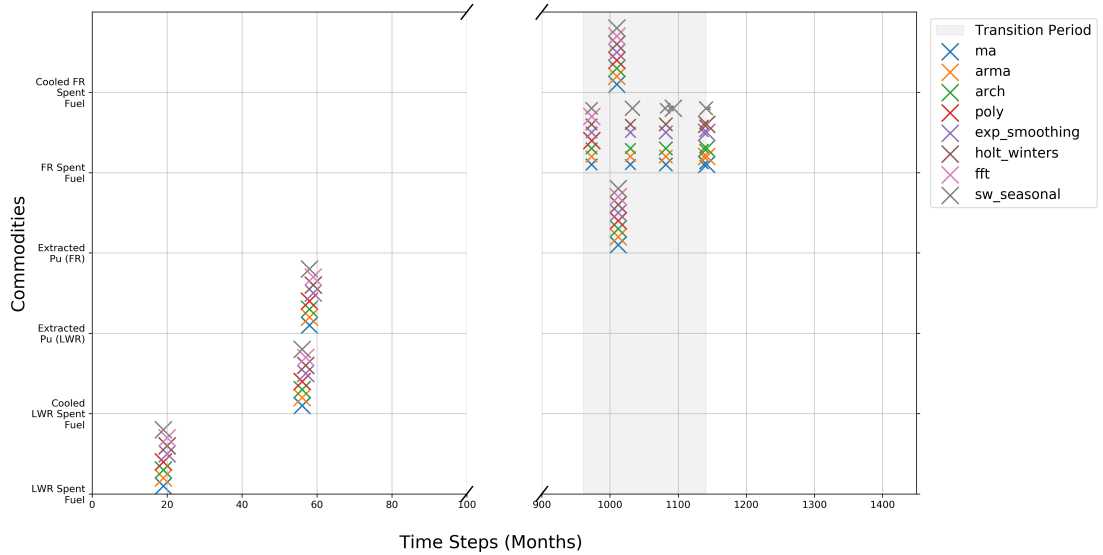
**Figure 4:** Facility and mass flow of the transition scenarios EG01-EG23 and EG01-EG29 in CYCLUS.

EG1-23: Time steps with an undersupply of each commodity for different prediction methods



(a) Time dependent undersupply of commodities in simulation

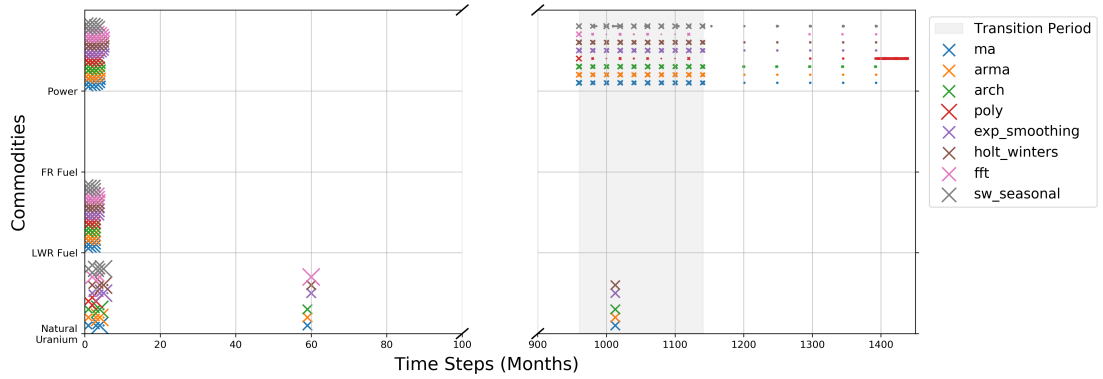
EG1-23: Time steps with an undercapacity of each commodity for different prediction methods



(b) Time dependent under-capacity of commodities in simulation

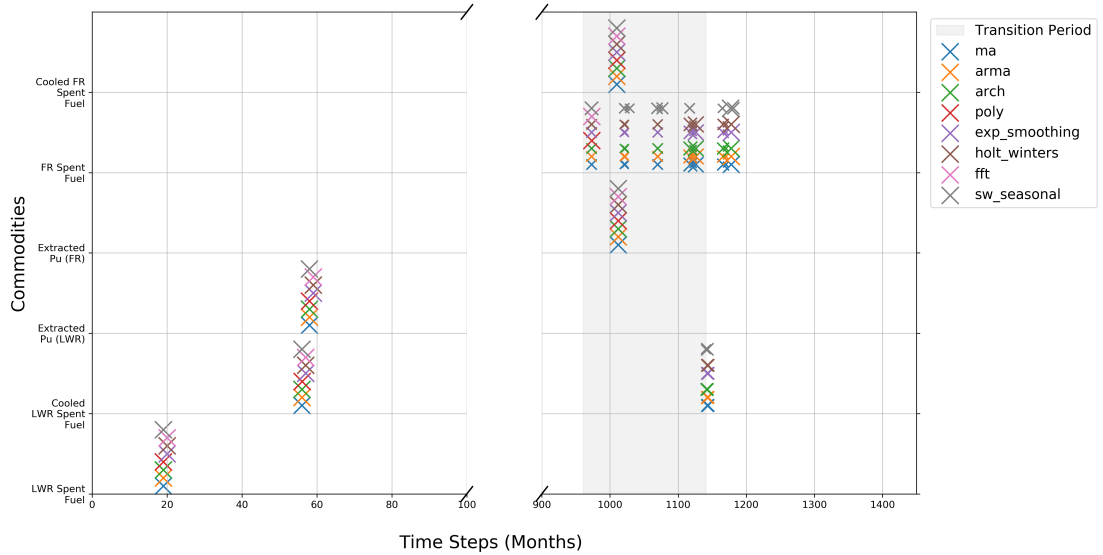
**Figure 5:** EG01-23 transition scenario with constant power demand. Each cross represents a time step in which there exists undersupply or under-capacity of each commodity for varying prediction methods. The size of each cross is proportional to the size of the undersupply.

EG1-24: Time steps with an undersupply of each commodity for different prediction methods



(a) Time dependent undersupply of commodities in simulation

EG1-24: Time steps with an undercapacity of each commodity for different prediction methods



(b) Time dependent under-capacity of commodities in simulation

**Figure 6:** EG01-24 transition scenario with linearly increasing power demand. Each cross represents a time step in which there exists undersupply or under-capacity of each commodity for varying prediction methods. The size of each cross is proportional to the size of the undersupply.

| Algorithm     | Power Undersupplied Time Steps |            |           |            |
|---------------|--------------------------------|------------|-----------|------------|
|               | EG01-EG23                      | EG01-EG24  | EG01-EG29 | EG01-EG30  |
|               | Constant                       | Linearly   | Constant  | Linearly   |
|               | Power                          | Increasing | Power     | Increasing |
|               |                                | Power      |           | Power      |
| MA            | 26                             | 36         | 15        | 24         |
| ARMA          | 26                             | 36         | 15        | 24         |
| ARCH          | 26                             | 36         | 15        | 21         |
| POLY          | 6                              | 65         | 4         | 9          |
| EXP-SMOOTHING | 27                             | 37         | 16        | 25         |
| HOLT-WINTERS  | 27                             | 37         | 16        | 25         |
| FFT           | 8                              | 20         | 5         | 9          |
| SW-SEASONAL   | 36                             | 107        | 14        | 51         |

**Table 4:** Undersupply and oversupply of power for EG01-EG23,24,29,30 transition scenarios for varying prediction methods.

### 3.3. Sensitivity Analysis

We conducted a sensitivity analysis of the power buffer size for the EG01-EG23, EG01-24, EG01-29, and EG01-30 transition scenarios. Varying the power buffer size does not impact the number of undersupply time steps for the EG01-EG23 and EG01-EG29 constant power demand transition scenarios with the POLY prediction method. In Table 7, there are 6 and 4 time steps in which there is power undersupply for the EG01-EG23 and EG01-29 transition scenarios, respectively. As seen in figure 5, these undersupply time steps occur at the beginning of the simulation and for one time step when the transition begins. We expected this since without time-series data at the beginning of the simulation, `d3ploy` takes a few time steps to collect time-series data about power demand to predict and start deploying reactor and supporting fuel cycle facilities. When the transition begins, power is undersupplied for one time step, following this, `d3ploy` accounts for the undersupply by deploying facilities to meet power demand. Therefore, we minimized the power undersupply for constant power EG01-EG23 and EG01-EG29 transition scenarios with a 0MW power supply

buffer.

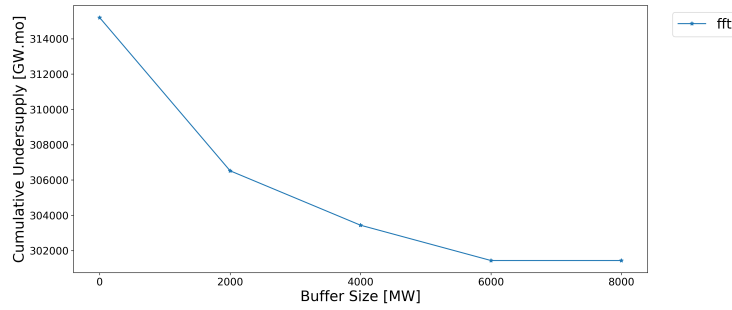
We varied the power buffer size for the EG01-24 and EG01-30 linearly  
 310 increasing power demand transition scenarios. Figures 7a, 7c, and Table 5  
 show that increasing the buffer size decreases the number of power undersupply  
 time steps. For EG01-24, the cumulative undersupply plateaus at 6000MW,  
 and for EG01-30, the cumulative undersupply is smallest for a buffer size of  
 8000MW. As seen from Figures 7b and 7d, these undersupply time steps occur  
 315 at the beginning of the simulation and for one time step when the transition  
 begins. We expected this since without time-series data at the beginning of  
 the simulation, `d3ploy` takes a few time steps to collect time-series data about  
 power demand to predict and start deploying reactor and supporting fuel cycle  
 facilities. Therefore, a buffer of 6000MW and 8000MW minimizes the power  
 320 undersupply for EG01-EG24 and EG01-EG30, respectively.

| Buffer [MW] | Undersupply              | EG01-24 | EG01-30 |
|-------------|--------------------------|---------|---------|
| <b>0</b>    | Time steps [#]           | 20      | 9       |
|             | Energy [ $GW \cdot mo$ ] | 315791  | 152517  |
| <b>2000</b> | Undersupplied [#]        | 9       | 6       |
|             | Energy [ $GW \cdot mo$ ] | 306520  | 147166  |
| <b>4000</b> | Time steps [#]           | 8       | 6       |
|             | Energy [ $GW \cdot mo$ ] | 303438  | 143166  |
| <b>6000</b> | Time steps [#]           | 7       | 5       |
|             | Cumulative [ $GW$ ]      | 303438  | 139083  |
| <b>8000</b> | Time steps [#]           | 7       | 5       |
|             | Energy [ $GW \cdot mo$ ] | 303438  | 135083  |

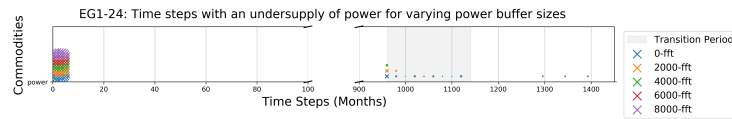
**Table 5:** The effect of sensitivity analysis of power buffer size on cumulative undersupply of power for EG01-EG24 and EG01-EG30 transition scenarios with linearly increasing power demand using the FFT prediction method.

### 3.4. Best Performance Models

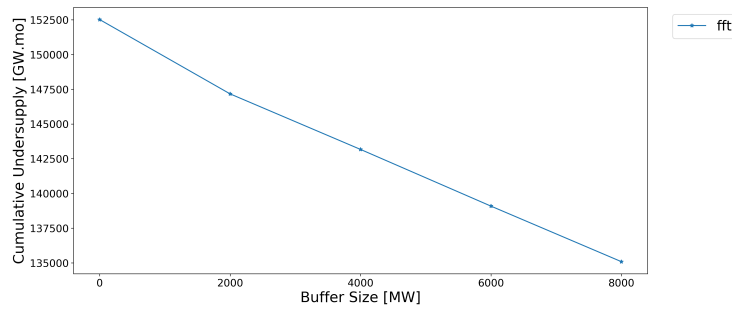
Table 6 shows the `d3ploy` input parameters for EG01-EG23, EG01-EG24, EG01-EG29, and EG01-EG30 transition scenarios that minimize the undersupply



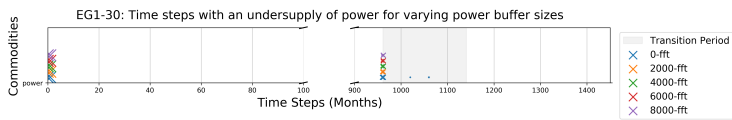
(a) EG01-24: Power buffer size vs. cumulative undersupply



(b) EG01-24: Time-dependent undersupply of power for varying power buffer sizes



(c) EG01-30: Power buffer size vs. cumulative undersupply



(d) EG01-30: Time-dependent undersupply of power for varying power buffer sizes

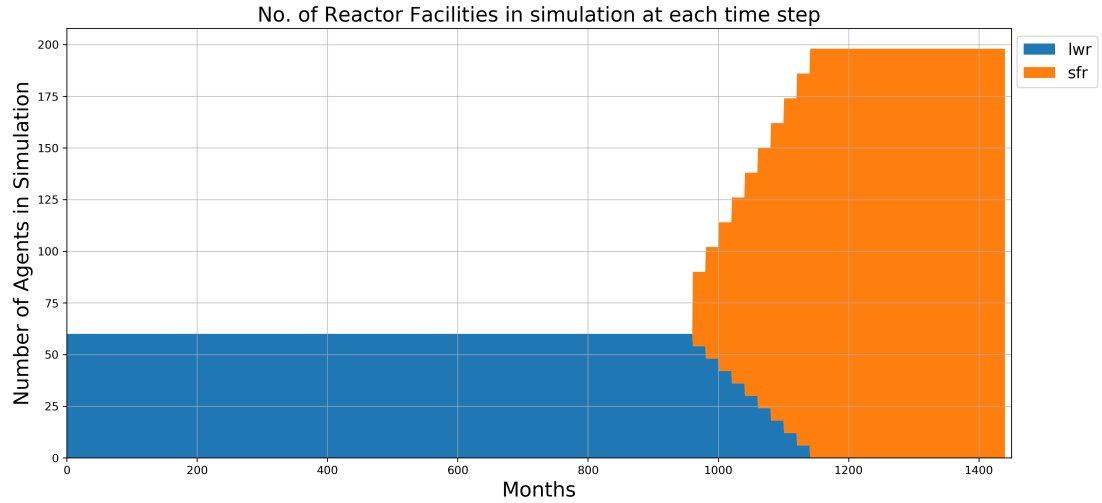
**Figure 7:** The effect of sensitivity analysis of power buffer size on cumulative undersupply of power for EG01-EG24 and EG01-EG30 transition scenarios with linearly increasing power demand using the FFT prediction method.

|                 | Input Parameter           | Simulation Description   |                 |         |                 |
|-----------------|---------------------------|--------------------------|-----------------|---------|-----------------|
|                 |                           | EG01-23                  | EG01-24         | EG01-29 | EG01-30         |
| <b>Required</b> | Demand driving commodity  | Power                    |                 |         |                 |
|                 | Demand equation [MW]      | 60000                    | 60000 + 250t/12 | 60000   | 60000 + 250t/12 |
|                 | Prediction method         | POLY                     | FFT             | POLY    | FFT             |
|                 | Deployment Driving Method | Installed Capacity       |                 |         |                 |
|                 | Fleet Share Percentage    | MOX LWR = 85%, SFR = 15% |                 |         |                 |
| <b>Optional</b> | Buffer type               | Absolute                 |                 |         |                 |
|                 | Power Buffer size [MW]    | 0                        | 6000            | 0       | 8000            |

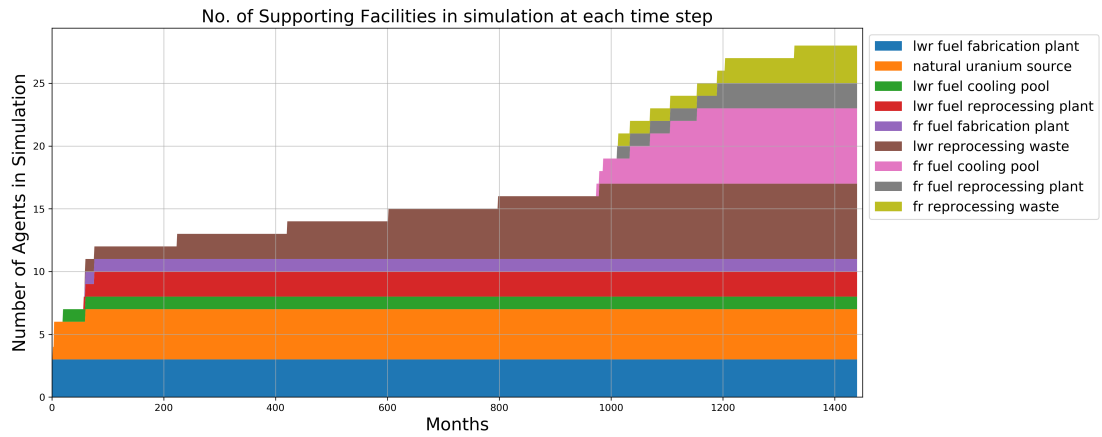
**Table 6:** d3ploy’s input parameters for EG01-EG23, EG01-EG24, EG01-EG29, and EG01-EG30 transition scenarios that minimizes undersupply of power and minimizes the undersupply and under-capacity of the other facilities.

of power and undersupply and under-capacity of the other commodities in the  
325 simulation. The need for commodity supply buffers is a reflection of reality in  
which a supply buffer is usually maintained to ensure continuity in the event of  
an unexpected failure in the supply chain.

Figures 8 and 9 show time-dependent deployment of reactor and supporting  
facilities for the EG01-23 constant power demand and EG01-30 linearly increasing  
330 power demand transition scenarios, respectively. d3ploy automatically deploys  
reactor and supporting facilities to set up a supply chain to meet power demand  
during a transition from LWRs to SFRs for EG01-23, and from LWRs to MOX  
LWRs and SFRs for EG01-30. EG01-24 and EG01-29 facility deployment plots  
are similar to EG01-23 and EG01-30, respectively, therefore they are not shown.



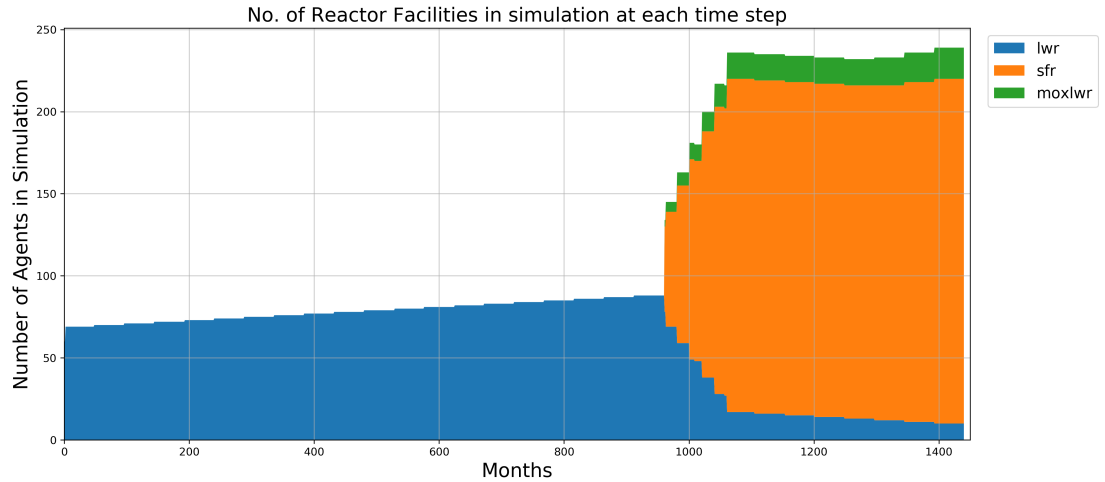
(a) EG01-23: Reactor Deployment



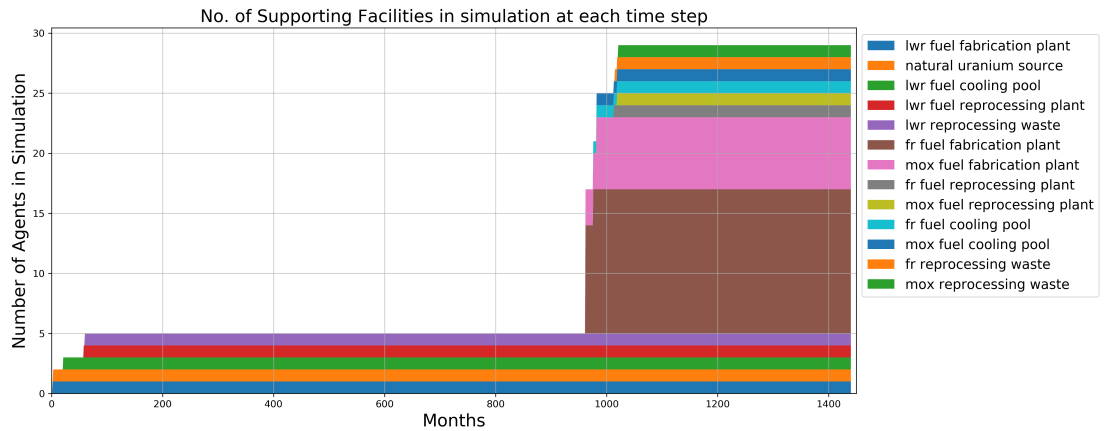
(b) EG01-23: Supporting Facility Deployment

**Figure 8:** Time dependent deployment of reactor and supporting facilities in the EG01-23 constant power demand transition scenario. `d3p1oy` automatically deploys reactor and supporting facilities to setup a supply chain to meet constant power demand of 60000 MW during a transition from LWRs to SFRs.





**(a)** EG01-30: Reactor Deployment



**(b)** EG01-30: Supporting Facility Deployment

**Figure 9:** Time dependent deployment of reactor and supporting facilities in the EG01-30 linearly increasing power demand transition scenario. d3ploy automatically deploys reactor and supporting facilities to setup a supply chain to meet linearly increasing power demand of  $60000 + 250t/12$  MW during a transition from LWRs to MOX LWRs and SFRs.

|                            | Undersupplied Time Steps |               |           |               |
|----------------------------|--------------------------|---------------|-----------|---------------|
| <b>Transition Scenario</b> | EG01-EG23                | EG01-EG24     | EG01-EG29 | EG01-EG30     |
| <b>Power Demand [MW]</b>   | 60000                    | 60000+250t/12 | 60000     | 60000+250t/12 |
| <b>Prediction Method</b>   | POLY                     | FFT           | POLY      | FFT           |
| <b>Power Buffer [MW]</b>   | 0                        | 6000          | 0         | 8000          |
| <b>Commodities</b>         |                          |               |           |               |
| Natural Uranium            | 2                        | 3             | 1         | 1             |
| LWR Fuel                   | 4                        | 6             | 1         | 2             |
| SFR Fuel                   | 0                        | 0             | 2         | 2             |
| MOX LWR Fuel               | -                        | -             | 2         | 2             |
| Power                      | 6                        | 7             | 4         | 5             |
| LWR Spent Fuel             | 1                        | 1             | 1         | 1             |
| SFR Spent Fuel             | 1                        | 1             | 1         | 1             |
| MOX LWR Spent Fuel         | -                        | -             | 1         | 1             |

**Table 7:** Undersupply/capacity of key commodities for the best performing EG01-EG23,24,29,30 transition scenarios.

#### 335 4. Conclusion

In this paper, we demonstrate that with careful selection of `d3ploy` parameters, we can effectively automate the setup of constant and linearly increasing power demand transition scenarios for EG01-23, EG01-24, EG01-29, and EG01-30 with minimal power undersupply. Using `d3ploy` to set up transition scenarios is more efficient than the previous efforts that required a user to manually calculate and use trial and error to set up the deployment scheme for the supporting fuel cycle facilities. Transition scenario simulations set up this way are sensitive to changes in the input parameters resulting in an arduous setup process since a slight change in one input parameter would result in the need to recalculate the deployment scheme to ensure no undersupply of power. Therefore, by automating this process, when the user varies input parameters in the simulation, `d3ploy` automatically adjusts the deployment scheme to meet the new constraints.

## 5. Future Work

We simulate transition scenarios to predict the future; however, when im-  
350 plemented in the real world, they tend to deviate from the optimal scenario.  
Therefore, NFC simulators must be used to conduct sensitivity analysis studies  
to understand the nuances of a transition scenario better to reliably inform  
policy decisions. [22]. Previously it was difficult to conduct sensitivity analysis  
with CYCLUS as users have to manually calculate the deployment scheme for a  
355 single change in an input parameter. By using the `d3ploy` capability, sensitivity  
analysis studies are more efficiently conducted to determine how variation in  
different input parameters impact the progress and final state of a transition  
scenario.

## 6. Acknowledgments

360 Department of Energy (DOE) Office of Nuclear Energy funds this research  
through the Nuclear Energy University Program (Project 16-10512, DE-NE0008567)  
'Demand-Driven Cyncamore Archetypes'. The authors want to thank members  
of the Advanced Reactors and Fuel Cycles (ARFC) group at the University  
of Illinois at Urbana-Champaign. Special thanks to Kip Kleimenhagen for his  
365 excellent proofreading help. We also thank our colleagues from the CYCLUS com-  
munity, particularly those in the University of Wisconsin Computational Nuclear  
Engineering Research Group (CNERG) and the University of South Carolina  
Energy Research Group (ERGS) for collaborative CYCLUS development.

## References

- 370 [1] A. M. Yacout, J. J. Jacobson, G. E. Matthern, S. J. Piet, A. Moiseyev,  
Modeling the Nuclear Fuel Cycle, in: The 23rd International Conference of  
the System Dynamics Society," Boston, Citeseer, 2005.  
URL [http://www.inl.gov/technicalpublications/Documents/  
3169906.pdf](http://www.inl.gov/technicalpublications/Documents/3169906.pdf)

- 375 [2] K. D. Huff, J. W. Bae, K. A. Mummah, R. R. Flanagan, A. M. Scopatz,  
Current Status of Predictive Transition Capability in Fuel Cycle Simulation,  
in: Proceedings of Global 2017, American Nuclear Society, Seoul, South  
Korea, 2017, p. 11.
- [3] K. D. Huff, M. J. Gidden, R. W. Carlsen, R. R. Flanagan, M. B. McGarry,  
380 A. C. Opotowsky, E. A. Schneider, A. M. Scopatz, P. P. H. Wilson,  
Fundamental concepts in the Cyclus nuclear fuel cycle simulation framework,  
Advances in Engineering Software 94 (2016) 46–59, arXiv: 1509.03604.  
doi:10.1016/j.advengsoft.2016.01.014.  
URL [http://www.sciencedirect.com/science/article/pii/  
385 S0965997816300229](http://www.sciencedirect.com/science/article/pii/S0965997816300229)
- [4] R. W. Carlsen, M. Gidden, K. Huff, A. C. Opotowsky, O. Rakhi-  
mov, A. M. Scopatz, P. Wilson, Cycamore v1.0.0, Figshare-  
Http://figshare.com/articles/Cycamore\_v1.0.0/1041829. doi:http://  
figshare.com/articles/Cycamore\_v1\_0\_0/1041829.  
390 URL [http://figshare.com/articles/Cycamore\\_v1\\_0\\_0/1041829](http://figshare.com/articles/Cycamore_v1_0_0/1041829)
- [5] Climate Change and Nuclear Power 2018, Non-serial Publications,  
INTERNATIONAL ATOMIC ENERGY AGENCY, Vienna, 2018.  
URL [https://www.iaea.org/publications/13395/  
climate-change-and-nuclear-power-2018](https://www.iaea.org/publications/13395/climate-change-and-nuclear-power-2018)
- 395 [6] Massachusetts Institute of Technology, The Future of nuclear power: an  
interdisciplinary MIT Study., MIT, Boston MA, 2003, oCLC: 53208528.
- [7] R. Wigeland, T. Taiwo, H. Ludewig, M. Todosow, W. Halsey, J. Gehin,  
R. Jubin, J. Buelt, S. Stockinger, K. Jenni, B. Oakley, Nuclear Fuel Cycle  
Evaluation and Screening - Final Report, US Department of Energy (2014)  
400 51.  
URL [https://fuelcycleevaluation.inl.gov/Shared%20Documents/  
ES%20Main%20Report.pdf](https://fuelcycleevaluation.inl.gov/Shared%20Documents/ES%20Main%20Report.pdf)

- [8] B. Feng, B. Dixon, E. Sunny, A. Cuadra, J. Jacobson, N. R. Brown, J. Powers, A. Worrall, S. Passerini, R. Gregg, Standardized verification of fuel cycle modeling, *Annals of Nuclear Energy* 94 (2016) 300–312. doi:10.1016/j.anucene.2016.03.002.  
URL <http://www.sciencedirect.com/science/article/pii/S0306454916301098>
- [9] G. Reikard, Predicting solar radiation at high resolutions: A comparison of time series forecasts, *Solar Energy* 83 (3) (2009) 342–349.
- [10] M. Diagne, M. David, P. Lauret, J. Boland, N. Schmutz, Review of solar irradiance forecasting methods and a proposition for small-scale insular grids, *Renewable and Sustainable Energy Reviews* 27 (2013) 65–76.
- [11] S. S. Soman, H. Zareipour, O. Malik, P. Mandal, A review of wind power and wind speed forecasting methods with different time horizons, in: *North American Power Symposium 2010*, IEEE, 2010, pp. 1–8.
- [12] J. W. Taylor, P. E. McSharry, R. Buizza, Wind power density forecasting using ensemble predictions and time series models, *IEEE Transactions on Energy Conversion* 24 (3) (2009) 775–782.
- [13] G. Chee, J. W. Bae, K. D. Huff, R. R. Flanagan, R. Fairhurst, Demonstration of Demand-Driven Deployment Capabilities in Cyclus, in: *Proceedings of Global/Top Fuel 2019*, American Nuclear Society, Seattle, WA, United States, 2019.
- [14] R. R. Flanagan, J. W. Bae, K. D. Huff, G. J. Chee, R. Fairhurst, Methods for Automated Fuel Cycle Facility Deployment, in: *Proceedings of Global/Top Fuel 2019*, American Nuclear Society, Seattle, WA, United States, 2019.
- [15] GitHub Community, *StatsModels: Statistics in Python Package* (2019).  
URL <https://www.statsmodels.org/stable/faq.html>
- [16] E. Jones, T. Oliphant, P. Peterson, *SciPy: Open source scientific tools for Python*, 2001, 2016.

- [17] N. Developers, NumPy, NumPy Numpy. Scipy Developers.
- [18] R. J. Hyndman, G. Athanasopoulos, Forecasting: principles and practice, OTexts, 2018.
- [19] pmdarima: ARIMA estimators for Python (2019).  
435 URL <https://www.alkaline-ml.com/pmdarima/>
- [20] arfc/d3ploy: A collection of Cyclus manager archetypes for demand driven deployment, 10.5281/zenodo.3464123 (Sep. 2019).  
URL <https://github.com/arfc/d3ploy>
- [21] G. Chee, G. T. Park, K. Huff, arfc/transition-scenarios : Validation of Spent  
440 Nuclear Fuel Output by Cyclus, a Fuel Cycle Simulator Code (Aug. 2018).  
doi:10.5281/zenodo.1401495.
- [22] S. Passerini, M. S. Kazimi, E. Shwageraus, A Systematic Approach to  
Nuclear Fuel Cycle Analysis and Optimization, Nuclear Science and Engi-  
neering 178 (2) (2014) 186-201. doi:10.13182/NSE13-20.  
445 URL <https://doi.org/10.13182/NSE13-20>